

Enhanced stability of G-quadruplexes from conformationally constrained *aep*-PNA backbone†

Nagendra K. Sharma^{*a} and Krishna N. Ganesh^b

Received 2nd August 2010, Accepted 16th September 2010

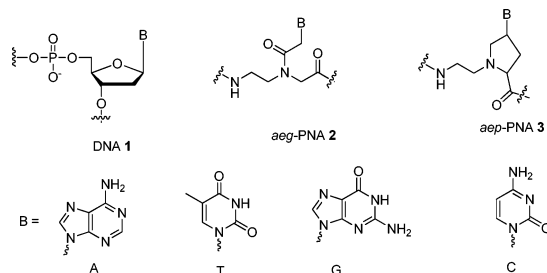
DOI: 10.1039/c0ob00528b

Nucleic (DNA) acids having contiguous stretch of G sequence form quadruplex structure, which is very critical to control cell division. Recently the existence of G-quadruplex in RNA is also reported in presence of monovalent metal ion. PNA is a promising DNA analogue which binds strongly to DNA to form PNA : DNA duplex or PNA₂ : DNA triplex. PNA also forms quadruplexes such G-quadruplex and *i*-motif in G and C-rich sequences respectively. *aep*-PNA containing a prolyl ring is one of several PNA analogues that provide rigidity and chirality in backbone and has binding affinity to natural DNA which is higher than that of PNA. Here we examine the ability of *aep*-PNA-G to form a quadruplex by UV, CD and mass spectroscopic techniques.

1. Introduction

DNA (deoxyribonucleic acid, **1**), the genetic material in living systems, has the natural structural property of forming sequence dependent self-assembled structures such as duplex, triplex and many other types of secondary structures through hydrogen bonding.¹ The G-rich sequence stretches of DNA exhibit a quadruplex structure, which occurs in chromosomal telomeres, immunoglobulin switch regions and regulatory regions of oncogenes.² The formation of such a G-quadruplex of DNA has a unique role in the cell division process.³ G-quadruplex structures have assumed importance in anticancer drug design,⁴ development of functional non-covalent assemblies such as G-wire,^{5,6} nanopore,⁷ ion-channels⁸ and self-assembled ionophores.⁹ Although quadruplexes arise essentially from inter- or intrastrand H-bonding between four guanine bases in DNA, formation of G-quadruplexes by DNA analogues or mimetics such as locked nucleic acid (LNA)¹⁰ and aminoethyl glycine (*aeg*) peptide nucleic acid (PNA, **2**)¹¹ are interesting to understand the role of the backbone in inducing the self assemblies. We have recently shown that the pH dependent *i*-motif formed by interdigitation of C : C⁺ self base pairing in DNA is also seen in PNA, but at slightly acidic pH due to the altered pK_a of N3 in C of PNA.¹² The G-quadruplex derived from aminoethyl glycine (*aeg*)-PNA is found to be more stable than that of DNA.¹³ To modify their

binding affinity and enhance selectivity and solubility, many PNA analogues have been designed and synthesized.¹⁴ One of our different rationales for modification of PNA comprised of introduction of chirality and rigidity in the backbone. During this process, we designed and studied aminoethylprolyl (*aep*) PNA (**3**) which is a positively charged, conformationally constrained chiral analogue that exhibited higher stability of its duplexes and triplexes with complementary DNA over that of the corresponding complexes of unmodified *aeg*-PNA.¹⁵ These features of conformationally constrained *aep*-PNA have prompted us to explore its G-quadruplexing properties. Herein we report the synthesis and quadruplex stability of G_n-*aep*-PNA (*n* = 2–4) sequences at different pH and salt concentrations to find that the *aep*-PNA derived quadruplexes have improved stability over that of unmodified PNA sequences.



2. Results and discussion

Synthesis of *aeg*- and *aep*-PNA oligomers

The *N*-Boc protected (2*S*,4*S*)-*aep*-PNA-T (**4**) and (2*S*,4*S*)-*aep*-PNA-G (**5**) monomers required for assembling the desired (2*S*,4*S*)-*aep*-PNA oligomers were synthesized starting from 4-hydroxyproline as per our earlier reported procedures.¹⁵ To prevent electrostatic repulsion, at the N-terminus of the shorter *aep*-PNAs

^aNational Institute of Science Education and Research (NISER) IOP Campus, P.O.: Sainik School, Bhubaneswar, 751005, Orissa, India. E-mail: nagendra@niser.ac.in; Tel: 91-674-230-4130, 91-674-230-4094

^bIndian Institute of Science Education and Research (IISER)-Pune 900, NCL Innovation Park, JC Bose Fellow, Division of Organic Chemistry, National Chemical Laboratory, Dr Homi Bhabha Road Pune, 411008, India. E-mail: kn.ganesh@iiserpune.ac.in; Fax: +91 20 2589 9790; Tel: +91 20 2590 8000

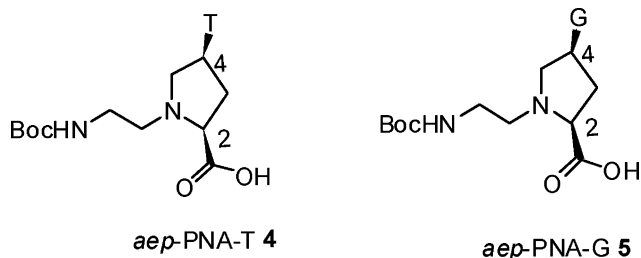
† Electronic supplementary information (ESI) available: Additional spectra. See DOI: 10.1039/c0ob00528b

Table 1 Sequence of *aeg*-/*aep*-PNA and DNA oligomers^a

PNA	Sequences PNA/DNA	Mass calc per strand	Obs. mass
P1	H ₂ N-T-G-G-G-T-β-ala	1786.7	1787.3
P2	H ₂ N-T-G-G-G-G-β-ala	1520.6	1520.4
P3	H ₂ N-T-G-G-g-G-t-β-ala	1784.7	1787.7
P4	H ₂ N-T-G-G-G-t-β-ala	1784.7	1786.2
P5	H ₂ N-t-g-g-g-t-β-ala	1774.9	1778.0
P6	AcHN-g-g-g-t-β-ala	1552.5	1553.0
P7	AcHN-g-g-t-β-ala	1263.3	1263.0
P8	AcHN-g-g-t-β-ala	974.0	931.9
P9	AcHN-g-t-β-ala	684.0	684.7

^a T and G – *aeg*-PNA, g and t – *aep*-PNA; DNA **D10** – d(5'-T-G-G-G-G-T-3') obtained from commercial sources

(**P6–P9**) the free amino groups were protected as acetates. For control studies, the required unmodified *aeg*-PNA-Thymine (T) and *aeg*-PNA-Guanine (G) monomers were synthesized by following literature procedures.¹¹ The G-rich oligomers of unmodified *aeg*-PNA (**P1**, **P2**) and *aep*-PNA (**P3–P8**, incorporating one or all modified *aep*-PNA-T and *aep*-PNA-G units) were synthesized by established solid phase peptide synthesis protocols.^{15,16} All PNAs were purified by HPLC and characterized by mass spectrometric (ESI/MALDI) methods (Table 1).



Biophysical studies of *aeg*-PNA and *aep*-PNA G-quadruplexes

A comparative study of quadruplex formation of various synthesized G-rich *aeg*- and *aep*-PNA sequences was done by temperature and salt dependent UV/CD-spectroscopy,¹⁷ isothermal titration calorimetry (ITC)¹⁸ and mass spectroscopic¹⁹ techniques.

The temperature dependent UV-profiles of *aep*-PNA (**P2–P9**) were recorded in potassium phosphate buffer (10 mM, pH 7.4) in the absence and presence of KCl (100 mM). Two broad peaks were observed in the spectra of both *aeg*-PNA (**P1–P4**) and *aep*-PNA (**P5–P8**) in the range 253–273 nm (Fig. 1). This pattern of UV spectra is indicative of formation of secondary structure and the results of Fig. 1 suggest that *aeg*-PNA and *aep*-PNA both form folded or complex structures from those PNA. The thermal stabilities of different G-quadruplexes from *aeg*-PNA, *aep*-PNA and DNA were measured by temperature dependent changes in UV absorbance monitored at 295 nm where the absorbance decrease due to increase in temperature is characteristic of the disassociation of G-quadruplex structure.^{20,21} The inverse sigmoidal nature of the UV-temperature profile at 295 nm (ESI†) due to the cooperative nature of transition confirmed the formation of quadruplexes. The apparent melting temperature T_m (temperature corresponding to mid-point of transition) obtained from the first derivative plots are shown in Table 2 for quadruplexes in potassium phosphate (10 mM) containing KCl (100 mM).

Table 2 UV- T_m (°C) of PNAs at different pHs^a

PNA	PNA sequence	pH 7.8	pH 7.0
P1	H ₂ N-T-G-G-G-T-β-ala	64.1	59.3
P2	H ₂ N-T-G-G-G-G-β-ala	63.1	63.4
P3	H ₂ N-T-G-G-G-g-t-β-ala	nd	62.5
P4	H ₂ N-T-G-g-g-G-t-β-ala	nd	62.4
P5	AcHN-t-g-g-g-t-β-ala	61.0	64.8
P6	AcHN-g-g-g-t-β-ala	59.2	63.5
P7	AcHN-g-g-g-t-β-ala	—	—
P8	AcHN-g-g-t-β-ala	—	—
P9	AcHN-g-t-β-ala	—	—

^a T and G – *aeg*-PNA, g and t – *aep*-PNA and D10 for DNA oligo. All T_m 's are average of 3 experiments and are accurate to ± 0.5 °C. All experiments were done in 10 mM Potassium Phosphate containing 100 mM KCl. nd denotes no detectable transition

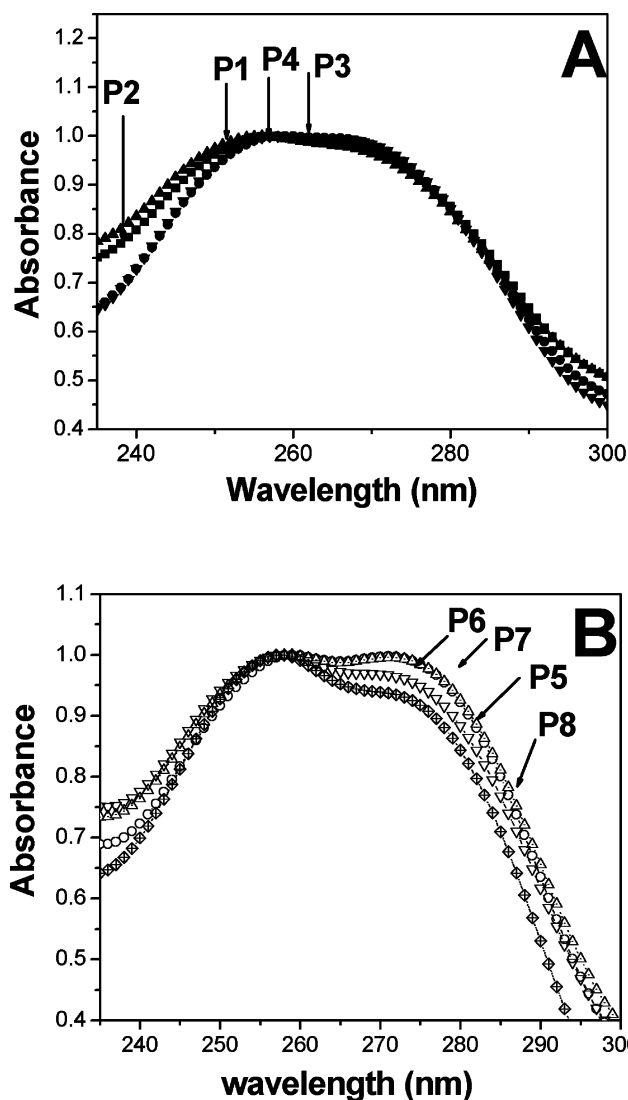


Fig. 1 UV-spectra of A. *aeg*-PNA (**P1** and **P2**), *aeg*-*aep*-PNA (**P3** and **P4**); B. *aep*-PNA (**P5**, **P6**, **P7** and **P8**) at 10 °C.

aep-PNAs are protonatable at the ring nitrogen at physiological pH, and hence their quadruplexing properties were examined at different pHs. UV-thermal melting profiles of PNA **P1**, **P3**, **P4** and **P5** at pH 7.4 are given in Fig. 2 and for all PNAs at

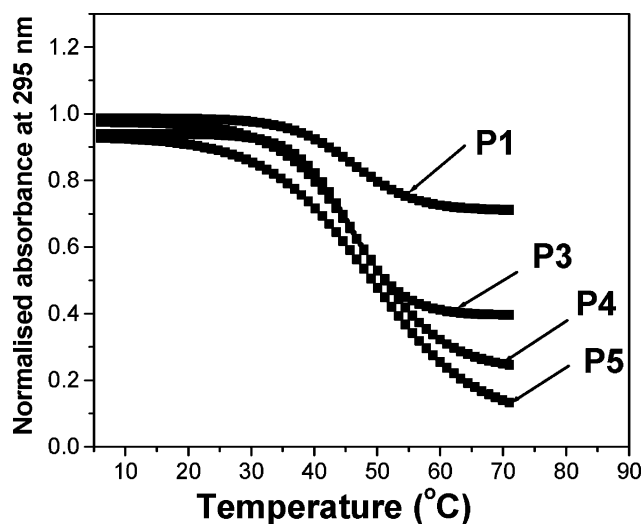


Fig. 2 UV-melting profile of *aeg*-PNA (**P1**) and *aep*-PNAs (**3–5**) in sodium phosphate (10 mM) at pH 7.4 and NaCl (100 mM).

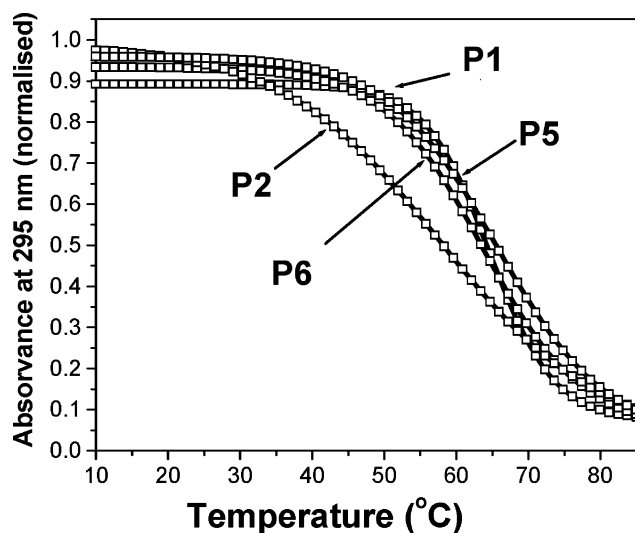


Fig. 3 UV-melting profile of *aeg*-PNA (**P1–P2**) and *aep*-PNA (**P5** and **P6**) in potassium phosphate (10 mM) and KCl (100 mM) at pH 7.4.

different pH are in Fig. 3–4 and ESI†. The T_m data extracted from the UV–temperature profile, indicate that modified *aep*-PNAs **P5** and **P6** form quadruplexes at pHs 7.0 like unmodified *aeg*-PNAs, with almost similar stability within the experimental error range. However at slightly higher pH of 7.8, *aep*-PNAs were destabilized by 3.0–3.5 °C compared to quadruplexes of unmodified *aeg*-PNAs. At slightly acidic pHs of 6.4 and 5.8, all PNAs showed multiple transitions, perhaps due to simultaneous existence of several complexes and even at pH < 5.8, no transitions were seen (data not shown). The shorter *aep*-PNA oligomers **P7–P9** showed no quadruplex formation under any conditions. Both *aeg*-PNA and *aep*-PNA G-tetraplexes formed stable quadruplexes compared to DNA D10 which did not show consistent evidence for quadruplex formation.

The stability of the G-quadruplex structure is known to depend on the type and concentration of metal ions (Na^+/K^+) that hold the two G-tetrads.⁸ Hence the T_m of *aeg*-PNA and *aep*-PNA G-quadruplexes was measured at different salt concentrations.

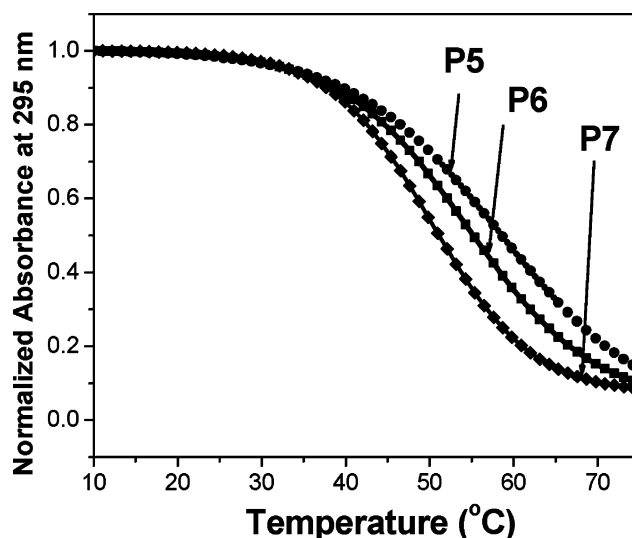


Fig. 4 UV-melting profile of *aep*-PNAs (**5–7**) under condition of potassium phosphate (10 mM) and KCl (100 mM) at pH 7.8. DNA melting curve removed.

The melting temperature obtained by addition of KCl (100 mM) enhanced the T_m of PNA quadruplexes **P1** to **P4** by 7 °C (Fig. 3), while for the all-modified *aep*-PNA **P5**, it was significantly about 14 °C. In comparison, in the presence of KCl (100 mM), UV-melting profiles of DNA **D10** were inconsistent. However increasing the metal ion concentration by enhancing the potassium buffer concentration to 100 mM had a much greater enhancement effect (>10 °C) on the T_m as compared to equivalent added salt concentration. The consequence was quite significant on both *aeg*-PNA and *aep*-PNA quadruplexes. The T_m values of PNA quadruplexes (**P1–P5**) in sodium phosphate buffer at pH 7.4 with NaCl (10 mM) reveal that the relative stabilities of *aep*-PNA **P5** and *aeg*-PNA G-quadruplex **P1** and DNA **D10** are almost same ($\approx \Delta T_m$ 1–2 °C) (Table 3, last column).

Introducing one modified *aep*-PNA-T or *aep*-G unit in the *aeg*-PNA backbone (**P3** and **P4**) destabilized the derived quadruplexes by $\Delta T_m \approx 1–4$ °C, as compared to unmodified quadruplex **P1** or fully modified quadruplex **P6** in potassium phosphate buffer (100 mM). The UV- $T_{1/2}$ results of Table 3 overall suggested that KCl stabilised PNA G-quadruplexes more than NaCl. Interestingly, the *aep* modification also led to enhancements in hypochromicity, with maximum effect (20%) seen with all-modified *aep*-PNA **P5**. The hypochromicity at 295 nm also generally increased with all PNAs (8–20%), perhaps suggesting a better stacking of G bases in *aep*-PNA.

In order to check the requirement of minimum length for G-quadruplexation, *aep*-PNAs **P5–P9** having 4, 3, 2 and 1 guanine were studied. In potassium phosphate (100 mM) containing KCl (100 mM), at two different pHs (7.4 and 7.8), only PNAs **P5**, **P6** and **P7** with 3 and 4 G residues exhibited characteristic quadruplex melting profiles shown in Fig. 3–Fig. 4. The T_m values (Table 2) of quadruplex of both **P5** and **P6** were higher than that of PNA **P7**. The short length *aep*-PNAs **P8** and **P9** failed to show quadruplex signature under any conditions. However PNA **P8** exhibited a duplex type transition (positive sigmoidal profile) and **P9** failed to show any transition (ESI†).

Table 3 UV- T_m ($^{\circ}\text{C}$) of *aeg*-PNA and *aep*-PNA G-quadruplexes at different concentration of salts^a

PNA/DNA	Sequences	KH_2PO_4 10 mM KCl (100 mM)	KH_2PO_4 100 mM	NaH_2PO_4 10 mM NaCl (100 mM)
P1	$\text{H}_2\text{N-T-G-G-G-G-T-}\beta\text{-ala}$	52.3 (64.0)	65.9	46.5
P2	$\text{H}_2\text{N-T-G-G-G-G-}\beta\text{-ala}$	47.0 (63.0)	56.4	45.3
P3	$\text{H}_2\text{N-T-G-G-g-G-T-}\beta\text{-ala}$	48.0 (56.4)	57.2	48.0
P4	$\text{H}_2\text{N-T-G-G-G-g-t-}\beta\text{-ala}$	48.0 (55.0)	56.3	47.6
P5	$\text{H}_2\text{N-t-g-g-g-g-t-}\beta\text{-ala}$	46.3 (61.0)	64.5	45.7
D10	$\text{d}(5'\text{-T-G-G-G-G-T-}3')$	nd ^a	nd ^a	45.5

^a T and G for *aeg*-PNA, g and t for *aep*-PNA and D10 for DNA oligo. All T_m s average 2–3 measurements and accurate within ± 0.5 $^{\circ}\text{C}$. All experiments were done at pH 7.4. Values in bracket are T_m values in the presence of 100 mM KCl. nd denotes no detectable transition

The CD-spectra of *aep*-PNAs of different lengths are shown in Fig. 5. From the literature, the CD spectrum of DNA **D10** shows maxima at 262 nm and minima at 238 nm, which is characteristic of an intermolecular G-quadruplex.²² The CD-spectra of *aep*-PNAs **P5–P8** show maxima at 271 nm and minima at 223 nm slightly different from that seen in G-quadruplex DNA. This difference suggests that in *aep*-PNA a different relative disposition of G-bases may result due to their direct linking to a pyrrolidine ring having nitrogen protonatable even at neutral pH. The present results do not yield any information on the relative parallel and antiparallel alignment of the four *aep*-PNA strands.

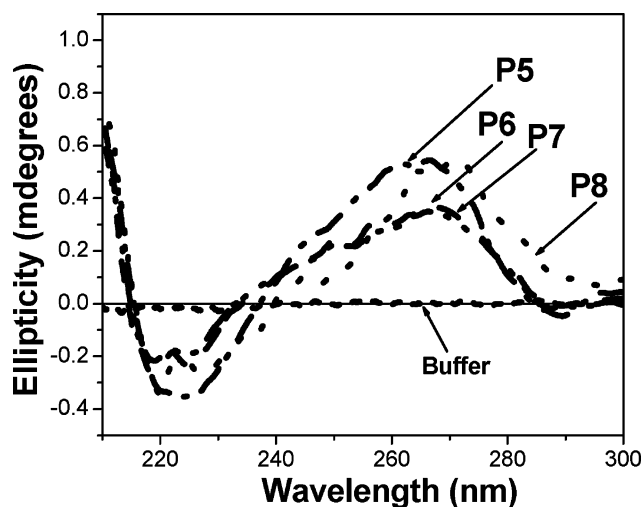


Fig. 5 CD-spectra of *aep*-PNAs in potassium phosphate (100 mM) and KCl (100 mM). Curves **P5**, **P6**, **P7**, and **P8** correspond to *aep*-PNAs.

Electrospray ionization mass spectrometry (ESI-MS) has recently been used to characterize quadruplexes of *aeg*-PNA-G and establish the molecularity of the PNA species.²³ In this context, we examined the ESI and MALDI-TOF spectra of *aep*-PNAs (ESI[†]). The expected mass peaks along with additional peaks derived from capture of Na^+ and K^+ ions were seen in the mass spectra. The observed M^+ from MALDI-TOF corresponding to quadruplex mass could be fitted into mass compositions of $(M_4+3\text{K}+\text{Na}+\text{H})^{5+}$ for *aep*-PNA **P1**, $(M_4+3\text{Na}+6\text{K}+\text{H})^{10+}$ for *aeg-aep*-PNA **P3** and $(M_4+\text{K}+3\text{H})^{4+}$ for PNA **P4** as evidence for the formation of G-quadruplexes in *aeg* and *aep*-PNAs. In *aep*-PNA **P6**, the mass spectrum (MALDI-TOF) exhibited the molecular ions of $(M+\text{H})^+ = 1553.58$, $(4M+2\text{Na}+2\text{H})^{4+} = 564.08$, $(M_4+4\text{Na})^{4+} = 575.1$, $(M_4+\text{Na}+3\text{K})^{4+} = 1588.0$, $(M+4\text{Na}+\text{H})^+ = 647.0$, $(M+4\text{Na}+\text{K})^+ = 1683.2$ which indicate the formation

of G-quadruplexes with one metal ion per tetrad composition (see ESI[†]). MALDI mass spectrum of PNA **P5** exhibited mass peaks as $M^{4+} = 1774.86$ corresponding to quadruplexes $(M_4+2\text{Na}+2\text{K})^+ = 7223.44$ and $(M_4+2\text{Na}+3\text{K}^+) = 7259.0$ which supported the formation of G-quadruplex. In ESI MS, mass peaks of *aep*-PNA **P5**, $M^{4+} = 1774.86$ corresponding to $(M_4+2\text{K}+\text{Na}+3\text{H}) = 1029.06$, $(M_4+2\text{K}+\text{Na}+3\text{H}) = 1050.92$ and $(M_4+4\text{K}+1\text{H})^{5+} = 1451.2$ are observed which supported the formation of G-quadruplexes.

Isothermal titration calorimetry

The process of quadruplex dissociation into single strands by dilution with buffer can be studied by isothermal titration calorimetry (ITC). The annealed and the un-annealed PNA quadruplexes were titrated (diluted) with buffer and the rate of change in the heat of dilution (dq/dt) was recorded at 20 $^{\circ}\text{C}$. The ITC plot dq/dt vs. the volume of titrant (buffer) for *aep*-PNA **P5** under G-quadruplexing condition exhibited characteristic pattern indicating heat evolution during the dilution of PNA-quadruplex. This was absent in samples that were not annealed (ESI[†] for additional data on PNAs *aeg-P1* and *aeg-aep-P3*). These preliminary data are insufficient to obtain any thermodynamic information at this stage, but nevertheless provide additional evidence for formation of G-quadruplex by *aep*-PNA.

3. Conclusions

The synthesis and characterization of quadruplexes from G-rich sequences of achiral *aeg*-PNA and chiral cationic *aep*-PNA are reported. The quadruplex structures are found to form in *aep*- and *aeg*-PNA under various conditions of pH, salt and metal ions K^+ and Na^+ . The stability of G-quadruplexes structure in *aep*-PNAs and equivalent *aeg*-PNA sequences stabilize the G-quadruplexes structures over DNA. The PNA quadruplexes are preferentially stabilized by K^+ in buffer and in salt conditions compared to Na^+ . The formation of quadruplexes is supported by mass spectroscopy, CD-spectra and ITC.

4. Experimental Section

The *aeg*- and *aep*-PNA monomers (T and G) synthesised by reported procedures were used to synthesize the PNA oligomers (**P1–P9**) by solid phase synthesis on Merrifield resin and purified by HPLC on C18 column. The concentrations of PNAs for different melting experiments were estimated by UV absorbance at λ 260 nm at 80 $^{\circ}\text{C}$, using molar extinction coefficient of

11700 cm⁻¹M⁻¹ for G and 8800 cm⁻¹M⁻¹ for T.²⁴ The UV melting experiments were performed on UV spectrometer equipped with Peltier temperature programmer and water circulator. Melting curves were recorded with concentration of single strand PNAs (10 μM) in appropriate buffer (2 mL) in Teflon-sealed quartz cuvettes (1 cm optical path length). The samples were annealed by heating at 80 °C for 15 min, followed by slow cooling and thermal equilibration at 20 °C for 20 min. UV absorption at λ₂₉₅ was monitored as a function of the temperature, heating at a rate of 0.5 °C min⁻¹. The results were analysed using software Origin 5.

The CD spectra were of PNAs **P5–P8** (5–10 μM) were recorded in phosphate buffer (100 mM, 2 ml) containing none or different salts (KCl or NaCl), annealed by heating at 90 °C for 5 min, followed by slow cooling to room temperature, kept for 30 min and refrigerated at 4 °C for 72 h. The CD spectra of the PNA samples were recorded at 10 °C using scanning speed of 200 nm min⁻¹ and addition of 5 scans. The electron spray ionization (ESI) mass spectra were recorded using samples of PNA (2 μM) in methanol (1 mL) and MALDI-TOF spectra were obtained using CHCA (α-cyano-4-hydroxycinnamic acid) matrix. For ITC experiments, the annealed PNA samples (10 μL) were successively titrated at 15 °C into the same buffer (1.5 mL) in a cell (250 μL) at intervals of 20 s.

Acknowledgements

NKS thanks UGC-CSIR for financial support. We are grateful to Dr Mahesh Kulkarni and Mrs Shantakumari (NCL, Pune) for assistance in mass spectroscopy. KNG acknowledges DST, New Delhi award of JC Bose fellowship. NKS also thanks the Department of Atomic Energy, Govt. of India for continuing his research work at NISER.

References

- 1 W. Saenger, *Principles of Nucleic Acid Structure*, Springer-Verlag, New York, 1984.
- 2 S. Neidle and S. Balasubramanian, *Quadruplex Nucleic Acids*, Royal Society of Chemistry, 2006.
- 3 S. Neidle and M. A. Read, *Biopolymers*, 2001, **56**, 195–220.
- 4 H. Y. Han and L. H. Hurley, *Trends Pharmacol. Sci.*, 2000, **21**, 136–142.
- 5 N. Smargiasso, F. Rosu, W. Hsia, P. Colson, E. S. Baker, M. T. Bowers, E. De Pauw and V. Gabelica, *J. Am. Chem. Soc.*, 2008, **130**, 10208–10216.
- 6 D. Miyoshi, A. Nakao and N. Sugimoto, *Nucleic Acids Res.*, 2003, **31**, 1156–1163.
- 7 X. Hou, W. Guo, F. Xia, F. Q. Nie, H. Dong, Y. Tian, L. P. Wen, L. Wang, L. X. Cao, Y. Yang, J. M. Xue, Y. L. Song, Y. G. Wang, D. S. Liu and L. Jiang, *J. Am. Chem. Soc.*, 2009, **131**, 7800–7805.
- 8 M. S. Kaucher, W. A. Harrell and J. T. Davis, *J. Am. Chem. Soc.*, 2006, **128**, 38–39.
- 9 S. L. Forman, J. C. Fettinger, S. Pieraccini, G. Gottarelli and J. T. Davis, *J. Am. Chem. Soc.*, 2000, **122**, 4060–4067.
- 10 L. Bonifacio, F. C. Church and M. B. Jarstfer, *Int. J. Mol. Sci.*, 2008, **9**, 422–433.
- 11 (a) S. Chakraborty, S. Modi and Y. Krishnan, *Chem. Commun.*, 2008, 70–72; (b) B. Datta and B. A. Armitage, *J. Am. Chem. Soc.*, 2001, **123**, 9612–9619; (c) E. A. Englund, Q. Xu, M. A. Witschi and D. H. Appella, *J. Am. Chem. Soc.*, 2006, **128**, 16456–16457; (d) U. Diederichsen, *Angew. Chem., Int. Ed.*, 1998, **37**, 2273–2276.
- 12 N. K. Sharma and K. N. Ganesh, *Chem. Commun.*, 2005, 4330–4332.
- 13 (a) Y. Krishnan-Ghosh, E. Stephens and S. Balasubramanian, *Chem. Commun.*, 2005, 5278–5280; (b) Y. Krishnan-Ghosh, E. Stephens and S. Balasubramanian, *J. Am. Chem. Soc.*, 2004, **126**, 5944–5945.
- 14 For review see: V. A. Kumar and K. N. Ganesh, *Acc. Chem. Res.*, 2005, **38**, 404–412.
- 15 (a) M. D'Costa, V. A. Kumar and K. N. Ganesh, *Org. Lett.*, 1999, **1**, 1513–1516; (b) M. D'Costa, V. Kumar and K. N. Ganesh, *Org. Lett.*, 2001, **3**, 1281–1284.
- 16 T. Kofoed, H. F. Hansen, H. Orum and T. Koch, *J. Pept. Sci.*, 2001, **7**, 402–412.
- 17 (a) J. B. Chaires, *FASEB J.*, 2010, **277**, 1098–1106; (b) C. C. Chang, C. W. Chien, Y. H. Lin, C. C. Kang and T. C. Chang, *Nucleic Acids Res.*, 2007, **35**, 2846–2860.
- 18 B. Pagano, A. Virno, C. A. Mattia, L. Mayol, A. Randazzo and C. Giancola, *Biochimie*, 2008, **90**, 1224–32.
- 19 (a) V. Gabelica, F. Rosu, M. Witt, G. Baykut and E. De Pauw, *Rapid Commun. Mass Spectrom.*, 2005, **19**, 201–208; (b) H. H. Li, Q. Zhang and G. Yuan, *Rapid Commun. Mass Spectrom.*, 2010, **24**, 393–395.
- 20 J. L. Mergny, J. Li, L. Lacroix, S. Amrane and J. B. Chaires, *Nucleic Acids Res.*, 2005, **33**, e138.
- 21 A. T. Phan and J. L. Mergny, *Nucleic Acids Res.*, 2002, **30**, 4618–4625.
- 22 S. Paramasivan, I. Rujan and P. H. Bolton, *Methods*, 2007, **43**, 324–331.
- 23 K. C. Gornall, S. Samosorn, J. Talib, J. B. Bremner and J. L. Beck, *Rapid Commun. Mass Spectrom.*, 2007, **21**, 1759–1766.
- 24 (a) K. L. Dueholm, K. H. Petersen, D. K. Jensen, M. Egholm, P. E. Nielsen and O. Buchardt, *Bioorg. Med. Chem. Lett.*, 1994, **4**, 1077–1080; (b) S. Modi, A. H. Wani and Y. Krishnan, *Nucleic Acids Res.*, 2006, **34**, 4354–4363.